HHS Public Access

Author manuscript

Circ Cardiovasc Imaging. Author manuscript; available in PMC 2019 March 01.

Published in final edited form as:

Circ Cardiovasc Imaging. 2018 March ; 11(3): e007007. doi:10.1161/CIRCIMAGING.117.007007.

Multiplexed Optical Imaging of Energy Substrates Reveals That Left Ventricular Hypertrophy Is Associated with Brown Adipose Tissue Activation

Marcello Panagia, MD DPhil[1,2,3], **Howard H. Chen, PhD**[2,3], **Dominique Croteau, BS**[1], **Yin-Ching Iris Chen, PhD**[3], **Chongzhao Ran, PhD**[3], **Ivan Luptak, MD PhD**[1], **Lee Josephson, PhD**[3], **Wilson S. Colucci, MD**[1], and **David E. Sosnovik, MD**[2,3]

[1]Cardiovascular Medicine Section, Department of Medicine, Boston University Medical Center, Boston, MA

[2]Cardiovascular Research Center, Massachusetts General Hospital, Boston, MA

[3]Martinos Center for Biomedical Imaging, Department of Radiology, Massachusetts General Hospital, Boston, MA

Abstract

Background—Substrate utilization in tissues with high energetic requirements could play an important role in cardiometabolic disease. Current techniques to assess energetics are limited by high cost, low throughput and the inability to resolve multiple readouts simultaneously. Consequently, we aimed to develop a multiplexed optical imaging platform to simultaneously assess energetics in multiple organs in a high throughput fashion.

Methods and Results—The detection of ^{18}FDG uptake via Cerenkov luminescence and free fatty acid (FFA) uptake with a fluorescent C_{16} FFA was tested. Simultaneous uptake of these agents was measured in the myocardium, brown/white adipose tissue (BAT/WAT) and skeletal muscle in mice with/without thoracic aortic banding (TAC). Within 5 weeks of TAC, mice developed left ventricular hypertrophy (LVH) and BAT activation with upregulation of β_3 adrenergic receptors and increased natriuretic peptide receptor ratio. Imaging of BAT 15 weeks post TAC revealed an increase in glucose ($p < 0.01$) and FFA ($p < 0.001$) uptake versus controls, and an increase in uncoupling protein-1 ($p < 0.01$). Similar but less robust changes were seen in skeletal muscle, while substrate uptake in WAT remained unchanged. Myocardial glucose uptake was increased post-TAC but FFA uptake trended to decrease.

Conclusions—A multiplexed optical imaging technique is presented that allows substrate uptake to be simultaneously quantified in multiple tissues in a high throughput manner. The activation of BAT occurs early in the onset of LVH, which produces tissue-specific changes in substrate uptake that may play a role in the systemic response to cardiac pressure overload.

Correspondence: David E. Sosnovik, MD, Martinos Center for Biomedical Imaging, Massachusetts General Hospital and Harvard Medical School, 149 13th St, Charlestown, MA 02129, VOICE: (617) 724-3407, sosnovik@nmr.mgh.harvard.edu.

Disclosures

None.

Keywords

Left Ventricular Hypertrophy; Heart Failure; Metabolism; Optical Imaging; Brown Adipose Tissue

Subject Terms

Metabolism; Imaging; Hypertrophy; Heart Failure

The regulation of substrate utilization and energy metabolism is of fundamental importance in tissues with high metabolic rates and abundant mitochondria, such as the heart and brown adipose tissue (BAT). Traditional metabolic imaging techniques such as positron emission tomography (PET) and magnetic resonance spectroscopy[1], while providing valuable insights, have several limitations including low throughput, high complexity, high cost and the inability to image multiple metabolic processes simultaneously. Optical imaging techniques can overcome many of these limitations and are being extensively used in cardiovascular investigation[2–5]. However, optical techniques, as of yet, have not been used to investigate energy metabolism in the heart or other tissues.

Changes in substrate utilization in the heart have been linked to adaptive, maladaptive and pathologic processes[6–9]. However, little is known about the changes in substrate metabolism in BAT and other systemic tissues in the setting of pathologic heart disease such as cardiac pressure overload. Recent studies have expanded the role of BAT from non-shivering thermogenesis to include whole body energy regulation, insulin sensitivity and neurohormonal signaling in heart failure[10,11]. The traditional mechanism for BAT activation has been through cold stimulation, likely mediated by the sympathetic nervous system and β_3 adrenergic receptors (β_3AR)[12,13], but recent work has shown that natriuretic peptides can also activate BAT[14].

The principal aim of the current study was to explore the influence of cardiac pressure overload and consequent left ventricular hypertrophy (LVH) on substrate uptake in the body. We hypothesized that a novel, multiplexed optical imaging approach, involving Cerenkov luminescence imaging (CLI) of glucose[15,16] and fluorescence imaging of free fatty acids (FFA), would allow substrate uptake in multiple tissues to be assessed in a relatively low cost and high throughput fashion. We further hypothesized that this technique would reveal changes in BAT metabolism in response to cardiac pressure overload and LVH.

METHODS

Mouse Model of Left Ventricular Hypertrophy

Left ventricular hypertrophy was induced by thoracic aortic banding in 10-week old female C57BL/6 mice (n = 25), as previously described[17]. In brief, after the chest was opened and aortic arch visualized, a 27-gauge needle was placed adjacent to the aorta. An 8-0 suture was then used to occlude the needle around the ascending aorta. After occlusion, the needle was removed, the chest closed and the animals were allowed to recover. Age matched healthy female C57BL6 mice (n=26) were used as controls. All surgical procedures were performed in accordance with animal protocols approved by the Institutional Animal Care and Use

Committee of Massachusetts General Hospital. The data, analytic methods, and study materials will not be made available to other researchers for purposes of reproducing the results or replicating the procedure.

Cardiac Phenotype by Magnetic Resonance Imaging after TAC

In vivo cardiac MRI was performed at 5 (n=9) and 15 weeks (n=8) after TAC to assess cardiac morphology and function. Gradient echo cine images were acquired at 9.4 Tesla (Biospec, Bruker, Billerica, MA) in the short axis of the left ventricle using cardiorespiratory gating (SA Instruments, Stonybrook, NY) as previously described[18,19], and with the following parameters: FOV 2.5 × 2.5 cm^2, slice thickness 1 mm, matrix, 192 × 192, flip angle 30°, 20 frames per R-R interval, TE 1.6 ms, 4 averages. Image analysis was performed using Osirix (v5.8.5). Ejection fraction was calculated using the Simpson's method of discs as previously described[20]. Similarly, the epicardial and endocardial borders were traced and the LV mass was calculated by the following equation: $\Sigma(LV_{epi}-LV_{endo})*1.05g/cm^3$.

PCR and Western Blotting

Separate cohorts of TAC mice were euthanized at 5 (n=4) and 15 weeks (n=4) to assess BAT morphology, weight and metabolic profile (control n=5 for both time points). The wet weight of tissues was measured and then snap frozen in liquid nitrogen. Samples were ground under liquid nitrogen and total RNA was extracted with an RNeasy Tissue Lipid Kit (Qiagen). Total RNA was converted to cDNA and quantitative PCR for key enzymes of BAT metabolism was performed[21] (see Supplement).

UCP1 protein levels in BAT were measured. Frozen BAT samples were homogenized in SDS lysis buffer. Equal amounts of total protein were separated by SDS-PAGE on 10% gels and transferred to PVDF membrane. UCP1 protein was detected using UCP1 primary antibody (Abcam) and normalized to αTubulin (Calbiochem) (see Supplement).

In Vitro Validation of Optical Signals

Calibration of the optical signals from ^{18}F-FDG and BODIPY-labeled free fatty acid analog BODIPY® FL C_{16} (4,4-Difluoro-5,7-Dimethyl-4-Bora-3a,4a-Diaza-s-Indacene-3-Hexadecanoic Acid) (Thermo Fisher Scientific) (FFA) was performed by imaging a range of known concentrations of each probe *in vitro* (see Supplement).

Ex Vivo Validation of Cerenkov Luminescence

Further validation of the Cerenkov luminescence signal was performed in mice (C57BL6, Jackson Laboratories, Bar Harbor, Maine) with myocardial infarction, providing very distinct areas of normal/abnormal myocardial metabolism. Myocardial infarction (MI) was induced in female C57BL6 mice (n=3) by coronary ligation, as previously described[18]. Two days post myocardial infarction, the mice were injected via the intraperitoneal (i.p.) route with 0.05 mCi/g of ^{18}F-FDG. The ^{18}F-FDG was allowed to circulate for 1 hour while the animals were active, after which time they were euthanized, the heart excised, sectioned and imaged with CLI. Following CLI, the sections were stained with triphenyltetrazolium chloride (TTC) and imaged using a conventional light stereomicroscope[22]. The percent

viable area by ^{18}F-FDG was correlated with the percent viable area by TTC for each slice (see Supplement).

Multiplexed Optical Imaging of Substrate Uptake

At 15 weeks post TAC, mice were simultaneously injected i.p. with 0.05 mCi/g of ^{18}F-FDG diluted in PBS and 1 nmol/g of Bodipy C_{16} FFA diluted in PBS, 7% DMSO and 4% fatty acid free BSA. Final volume of injection for each probe was 100 μL. Total *in vivo* circulating time for ^{18}F-FDG was 60 minutes and 30 minutes for Bodipy C_{16} FFA. Animals were subsequently euthanized and tissues were harvested. Intrascapular BAT was dissected from surrounding WAT using a light microscope. Whole hearts were sectioned into short-axis slices (3–4 slices per heart). Epididymal WAT and quadriceps skeletal muscle were also harvested. The tissues were immediately washed in ice cold PBS and imaged using the IVIS Spectrum imaging system (see Supplement).

Analysis of the optical images was performed using the Living Image v4.5 software package (PerkinElmer, Boston, MA). A region of interest (ROI) was drawn manually around the tissues. Radiance (photons/second/cm^2/sr) was calculated for ^{18}F-FDG and radiant efficiency (radiance/μW/cm^2) was calculated for Bodipy C_{16} FFA. An equivalently sized ROI was drawn adjacent to the tissue and served as the background signal, which was subtracted from the average radiance (AR) and average radiant efficiency (ARE).

In Vivo Cerenkov Luminescence Imaging of the Heart

Female nu/nu mice (n=5) were anesthetized with isoflurane balanced with oxygen for 5 minutes and injected with either saline (control) or ^{18}F-FDG (250 μCi, n=4) intravenously via the tail vein. Luminescence imaging was performed in the mice 30 minutes after ^{18}F-FDG injection with the following parameters: open filter, F-stop = 1, binning = 4, FOV = 22 × 22 cm^2, and exposure time = 120 s. Smoothing (3×3) was performed post-image acquisition.

Statistical Analysis

Comparison between 2 groups was performed with either a Mann-Whitney test or unpaired t-test based on the normality of the data. Comparison between greater than two groups was performed with ANOVA and a Tukey's post-test comparison. Two-tailed probability values are reported and statistical significance is defined as $p<0.05$. Correlations, when appropriate, were performed using Spearman correlation. Values are reported as mean ± standard deviation (SD). All statistical analyses were performed using Prism v6.0 (Graphpad Software Inc. LaJolla, CA).

RESULTS

Cardiac Phenotype

At 5 weeks post-TAC, LV mass was increased by 35% compared to age matched controls ($p < 0.05$), whereas end diastolic volume (EDV), end systolic volume (ESV) and ejection fraction (EF) were not different (Figure 1). At 15 weeks post-TAC, LV mass was also increased by 38% compared to age matched controls ($p < 0.05$; Figure 1). There was no

difference in LV mass at 5 weeks post-TAC compared to 15 weeks post-TAC. At 15 weeks post-TAC, EDV remained stable, whereas ESV trended upward in the banded animals. A significant reduction in EF ($p < 0.05$; Figure 1) was seen between the banded mice at 15 weeks and 5 weeks, as well as between banded mice and age matched control mice. Consistent with the MRI mass measurements, heart weight was increased 5 weeks post-TAC and remained stable at 15 weeks (Figures 2A and 3A, respectively). Thus, as is typical of this model, aortic banding led to LVH by 5 weeks and a progression to mild systolic dysfunction by 15 weeks.

BAT Phenotype 5 Weeks Post-TAC

At 5 weeks there were no significant differences in body weight (24 ± 1 g vs 22 ± 1 g) or BAT wet weight between control and banded animals (Figure 2B). Quantitative RT-PCR showed a 2.5× increase in mRNA expression for the β_3-adrenergic receptor (β_3AR) in BAT from banded mice ($p = 0.032$) and a 48% decrease ($p = 0.016$) in the natriuretic peptide clearance receptor (NPRc) (Figure 2C). There was no significant change in the natriuretic peptide active receptor (NPRa) in BAT, but the NPRa/c ratio, which determines the natriuretic peptide bioactivity in a tissue[11,23], was increased 2.8-fold ($p = 0.005$) in the BAT of banded animals. These receptor changes suggest BAT was activated in banded animals. However, downstream to these receptors, only fatty acid transporter 1 (FATP1) mRNA was increased (1.8×) in banded mice ($p = 0.006$; Figure 2E) whereas the mRNA levels for several of the remaining key enzymes involved in FFA and glucose handling were not different (all $p > 0.05$) in BAT from control vs banded animals, including: carnitine palmitoyltransferase 1b (CPT1B), medium-chain acyl-CoA dehydrogenase (MCAD), glucose transporter 1 (GLUT1), glucose transporter 4 (GLUT4) and pyruvate dehydrogenase kinase 4 (PDK4) (Panels 2E and F). A non-significant decrease in UCP1 mRNA was seen at 5 weeks (data not shown), in agreement with a recent report[24]. However, UCP1 protein abundance was unchanged in banded animals (Figure 2D) ($p = 0.62$). Thus, at 5 weeks post-TAC, there was little evidence of a change in the downstream metabolic profile in BAT, and accordingly, optical imaging of substrate uptake was deferred until 15 weeks post-TAC.

BAT Phenotype 15 Weeks Post-TAC

By 15 weeks post-TAC, BAT wet weight in banded mice had decreased by 40% ($p = 0.0001$) vs control animals (Figure 3), while there was no difference in body weights (25 ± 1 g vs 23 ± 1 g) between the two groups. Similar to 5 weeks post-TAC, there was a 2.5× increase in mRNA for β_3AR in BAT from banded mice ($p = 0.004$), although the increase in the NPRa/c ratio no longer reached significance (Figure 3) ($p = 0.3$). Similar to the 5-week time point, FATP1 was increased (2.1×) at the 15 week time point in banded animals ($p = 0.003$). However, in contrast to 5 weeks post-TAC, there was also a 20% increase in MCAD mRNA ($p = 0.04$), a 71% increase in GLUT4 mRNA ($p = 0.002$) and a trend towards increased CPT1B mRNA expression (Panels 3E and F). Moreover, at 15 weeks, there was a 2-fold increase ($p = 0.010$) in the quantity of UCP1 protein in BAT from banded vs control animals (Figure 3D). Thus, by 15 weeks post-TAC there was evidence of increased BAT metabolism as reflected by upregulation of enzymes involved in both glucose and fat metabolism, and increased abundance of UCP1. All optical imaging was therefore performed at this time point.

Calibration and Validation of Optical Imaging Platform

Prior to applying the optical imaging platform to the TAC model of LVH, *in vitro* and *ex vivo* analyses were performed. There was an excellent correlation ($R^2 = 0.99$) between ^{18}F-FDG activity and the AR measured optically (CLI) (Supplemental figure 1A). Similarly, the concentration of Bodipy C_{16} FFA also showed an excellent correlation ($R^2 = 0.97$) with the fluorescence intensity measured as ARE (Supplemtental figure 1B). Myocardial infarction caused by ligation of the left coronary artery resulted in a typical 'crescent' shaped infarct zone, which did not accumulate ^{18}F-FDG while the viable remote zone did. This was visualized with CLI and TTC (Supplemental figure 1C and D), and a high level of correlation ($R^2 = 0.9$, $p < 0.001$) was seen (Supplemental figure 1E).

Optical Imaging of Substrate Uptake

Multiplexed optical imaging, performed at 15 weeks post–TAC, showed a 70% increase in glucose uptake in the hearts of banded vs control animals (Figure 4A) ($p = 0.011$). Although there was a trend towards lower FFA uptake in the hearts from banded animals, this did not reach significance ($p = 0.5$). Glucose uptake in BAT in the 15-week banded mice was 2.7-fold higher compared to BAT from control mice (Figure 4B) ($p = 0.002$); and there was a 1.9-fold increase in FFA uptake (Figure 4B) ($p = 0.0004$). Skeletal muscle from banded animals showed a pattern that was similar but less robust than BAT with a 33% increase in glucose uptake ($p = 0.022$) and a 2-fold increase in FFA uptake (Figure 5A) ($p = 0.041$). In contrast to the pattern in BAT, there were no significant differences in glucose or FFA uptake in WAT (Figure 5B). Four distinct, and tissue-specific, metabolic patterns were thus detected in the banded mice at 15 weeks, as summarized in the Table. Absolute values for the optical readouts above are provided in the Supplement (Supplemental Table 1).

In Vivo Cerenkov Luminescence Imaging

CLI could be successfully performed in all 5 mice. Mice injected with saline did not exhibit any luminescence (Figure 6A) whereas a robust signal was visible in the upper thorax of all mice injected with ^{18}F- FDG (Figure 6B) consistent with cardiac glucose uptake.

Discussion

Optical imaging approaches have been extensively used to study cell biology in the cardiovascular system[4,5] but have hitherto not been applied to study energetics or metabolism in whole organs. Here we describe an approach based on Cerenkov luminescence to study multiple metabolic processes and organs in a high throughput manner. This multiplexed technique allowed glucose and FFA uptake, in a model of LVH, to be simultaneously assessed in the myocardium, BAT, WAT and skeletal muscle. The increase in glucose and FFA uptake observed in BAT during the transition from LVH with a preserved to reduced EF suggests that altered substrate metabolism in BAT could be a feature associated with advanced LVH.

Fluorescence imaging of glucose uptake has previously been attempted with molecules such as 2-NBDG (2-(N-(7-Nitrobenz-2-oxa-1,3-diazol-4-yl)amino)-2-Deoxyglucose[25]. However, the transport kinetics of these agents are likely governed by the bulky, hydrophobic

fluorophore, rather than the small hydrophilic glucose molecule itself[26]. In contrast, ^{18}F-FDG is inert and has been used extensively to assess glucose uptake with PET. While the current study was limited to the imaging of glucose and free fatty acids, conceptually 4–5 spectrally resolvable substrates could be imaged simultaneously with this approach. While imaging in the current study was performed *ex vivo* to demonstrate proof-of-principle, our approach is well suited to *in vivo* imaging with fluorescence tomography (FMT). As an initial step in this direction, we show that Cerenkov images of FDG uptake in the mouse heart can be acquired *in vivo*. Efforts to combine this with fluorescence imaging of fatty acid uptake *in vivo* are currently underway. This will allow the relevance of altered substrate uptake to be imaged, with our approach, under the full range of physiological conditions relevant to clinical pathophysiology including LVH and heart failure with reduced and preserved ejection fraction.

The identification of depots of BAT in adult humans has prompted interest in its role in human physiology[27,28]. Recent studies have suggested that communication between the heart and BAT is possibly mediated through sympathetic stimulation and natriuretic peptides[11–14]. In addition, there may be reciprocal communication between BAT and the heart, as BAT has been shown to modulate cardiomyocyte injury[29]. Magnetic resonance imaging produces strong endogenous contrast in BAT, allowing it to be imaged and differentiated from WAT[30]. Moreover, our group recently showed, using functional MRI techniques, that BAT is activated in a murine model of heart failure with reduced ejection fraction and that this activation consumes internal BAT lipid stores. This resulted in a decrease in BAT volume, as measured by MRI, and smaller lipid droplets in BAT measured by histology[20]. Here, we extend these physiologic observations and show that BAT is similarly activated in a model of LVH with a similar reduction in BAT mass. The pattern of BAT activation, however, was highly influenced by the duration of hypertrophy and the transition from a preserved to reduced ejection fraction.

The response of the heart to TAC can vary depending on animal strain, gender and surgical technique[31,32]. In the current study, at 5 weeks post-TAC, the mice showed signs of LV hypertrophy but preserved cardiac function by MRI. However, at 15 weeks post-TAC, many of the mice began showing signs of mild dysfunction with decreased EF. Despite no sign of decompensation at the 5-week time point, an increase in the upstream receptors responsible for BAT activation (increased β_3AR and increased NPRa/c ratio) was seen, suggesting that BAT signaling was affected by TAC physiology. In a recent report, changes in β_3AR mRNA in BAT were not observed 6 weeks post TAC[24], however differences in gender and technique may account for this difference. Increases in β_3AR as well as the NPRa/c ratio have been shown to occur in ‘beiging’ of WAT[33,34], and our data suggest that a similar phenomenon may occur early in the process of chronic BAT activation associated with LVH. However, this early activation of BAT was not associated with downstream changes in mRNA of most of the key enzymes involved in substrate utilization (apart from FATP1), BAT weight or UCP1 protein levels.

At 15 weeks post TAC, consistent with traditional concepts of increased BAT activity, UCP1 protein was significantly increased[35,36]. In addition, markers of increased uptake and handling of FFA (FATP1, CPT1B and MCAD) trended up or were significantly increased

and markers of glucose uptake (GLUT4) were also significantly increased. Although the enzymes selected for analysis were not an exhaustive list of potential mediators of substrate utilization, these data corroborated our imaging findings, which showed an increase in both glucose and FFA uptake in BAT at 15 weeks. Further studies examining protein expression, enzyme activity and phosphorylation states of the enzymes involved in glucose and fatty acid metabolism in BAT will be required to fully understand the signaling mechanisms. The activation of BAT in LVH may be adaptive or maladaptive and will also require further study. Increased BAT activity could provide a mechanism for cardiac cachexia, which is frequently seen in patients with end stage heart failure[37].

The changes we observed in myocardial substrate uptake have been well described in diseased myocardium[9,38–42], and further validate our optical approach. To the best of our knowledge, this is the first description of altered substrate uptake in BAT during LVH, which resembles the response of BAT to cold stimulation[43]. The elevation in UCP1 seen 15 weeks post-TAC strongly suggests that the increased substrate uptake is being utilized for uncoupled respiration in activated BAT. However, a limitation of all labeled imaging substrates is the inability to differentiate uptake from utilization. Hyperpolarized MRI holds significant promise in this regard and its strengths/limitations are highly complimentary to the high throughput optical approach we describe here. The breadth of our approach allowed us to identify major differences in the response of BAT, skeletal muscle and WAT to TAC. Our results are consistent with recent data suggesting that BAT and skeletal muscle have cell lineage progenitors in common and with different proteomic profiles than WAT[44,45].

In conclusion, a new platform to simultaneously study several aspects of substrate uptake and energy metabolism is presented. This multiplexed approach leverages the strength of optical imaging to examine multiple processes in multiple tissues in a simple and high throughput fashion. While the use of PET and MR spectroscopy will remain vital in human translation[46], they are complex techniques and are less suited to high-throughput preclinical studies. The multiplexed optical approach described here provides a rapid and broad assay of energetics in all metabolically active tissues in the body, the value of which is demonstrated by the detection of altered BAT metabolism in LVH. Further study of this phenomenon is warranted to define more fully the role of BAT activation at different stages of heart failure and its potential interaction with the heart.

Clinical Perspective

Energy substrate metabolism plays an important role in tissues with high energetic requirements and has been shown to be integral in heart failure pathogenesis. Interest in brown adipose tissue (BAT), an organ with abundant mitochondria and a high metabolic rate, has grown significantly since depots of BAT have been observed in adult humans and its role in whole body metabolic health is an active area of exploration. However, the ability to assay energy substrate metabolism in such tissues in rodents and humans has been hindered by high cost and low throughput techniques. Optical imaging techniques can overcome many of these limitations and have been explored in preclinical and clinical contexts. Recent studies have implied a relationship between heart function and BAT activation. In this study we use a combination of optical techniques to show, for the first time, that energy substrate uptake is

increased in BAT in a mouse model of left ventricular hypertrophy suggesting that BAT is activated with cardiac dysfunction. Clinically, these observations are important as cardiac cachexia is a hallmark of end stage heart failure, despite adequate nutritional intake, and portends a poor outcome. Chronic activation of BAT in heart failure may provide some insight into this process. The optical imaging approach to energy metabolism in this study is of value because it describes a useful pre-clinical tool to broadly assay energy substrate uptake in multiple tissues in a high throughput fashion thus allowing for quick and robust exploration of pre-clinical therapies on energy metabolism.

Supplementary Material

Refer to Web version on PubMed Central for supplementary material.

Acknowledgments

Dr. Panagia would like to thank Boston University School of Medicine for its support in the form of the Department of Medicine Career Investment Award.

Sources of Funding

This research was supported by the following National Institutes of Health grants: K08 HL123744-03 (M.P.), R01 HL093038 (D.E.S.), R01 HL112831 (D.E.S.), R01 HL064750 (W.S.C.), N01 HV28178 (W.S.C.)

References

1. Gupta A, Chacko VP, Schär M, Akki A, Weiss RG. Impaired ATP kinetics in failing in vivo mouse heart. Circulation: Cardiovascular Imaging. 2011; 4:42–50. [PubMed: 20926788]
2. Cao F, Lin S, Xie X, Ray P, Patel M, Zhang X, Drukker M, Dylla SJ, Connolly AJ, Chen X, Weissman IL, Gambhir SS, Wu JC. In vivo visualization of embryonic stem cell survival, proliferation, and migration after cardiac delivery. Circulation. 2006; 113:1005–1014. [PubMed: 16476845]
3. Mulder WJM, Griffioen AW, Strijkers GJ, Cormode DP, Nicolay K, Fayad ZA. Magnetic and fluorescent nanoparticles for multimodality imaging. Nanomedicine (Lond). 2007; 2:307–324. [PubMed: 17716176]
4. New SEP, Aikawa E. Molecular imaging insights into early inflammatory stages of arterial and aortic valve calcification. Circulation Research. 2011; 108:1381–1391. [PubMed: 21617135]
5. Burridge PW, Li YF, Matsa E, Wu H, Ong S-G, Sharma A, Holmström A, Chang AC, Coronado MJ, Ebert AD, Knowles JW, Telli ML, Witteles RM, Blau HM, Bernstein D, Altman RB, Wu JC. Human induced pluripotent stem cell-derived cardiomyocytes recapitulate the predilection of breast cancer patients to doxorubicin-induced cardiotoxicity. Nature Medicine. 2016; 22:547–556.
6. Panagia M, Gibbons GF, Radda GK, Clarke K. PPAR-alpha activation required for decreased glucose uptake and increased susceptibility to injury during ischemia. Am J Physiol Heart Circ Physiol. 2005; 288:H2677–83. [PubMed: 15665064]
7. Kolwicz SC, Olson DP, Marney LC, Garcia-Menendez L, Synovec RE, Tian R. Cardiac-specific deletion of acetyl CoA carboxylase 2 prevents metabolic remodeling during pressure-overload hypertrophy. Circulation Research. 2012; 111:728–738. [PubMed: 22730442]
8. Lai L, Leone TC, Keller MP, Martin OJ, Broman AT, Nigro J, Kapoor K, Koves TR, Stevens R, Ilkayeva OR, Vega RB, Attie AD, Muoio DM, Kelly DP. Energy metabolic reprogramming in the hypertrophied and early stage failing heart: a multisystems approach. Circulation: Heart Failure. 2014; 7:1022–1031. [PubMed: 25236884]
9. Taegtmeyer H, Young ME, Lopaschuk GD, Abel ED, Brunengraber H, Darley-Usmar V, Rosiers Des C, Gerszten R, Glatz JF, Griffin JL, Gropler RJ, Holzhuetter H-G, Kizer JR, Lewandowski ED, Malloy CR, Neubauer S, Peterson LR, Portman MA, Recchia FA, Van Eyk JE, Wang TJ. American

Heart Association Council on Basic Cardiovascular Sciences. Assessing Cardiac Metabolism: A Scientific Statement From the American Heart Association. Circulation Research. 2016; 118:1659–1701. [PubMed: 27012580]

10. Stanford KIK, Middelbeek RJWR, Townsend KLK, An DD, Nygaard EBE, Hitchcox KMK, Markan KRK, Nakano KK, Hirshman MFM, Tseng Y-HY, Goodyear LJL. Brown adipose tissue regulates glucose homeostasis and insulin sensitivity. J Clin Invest. 2013; 123:215–223. [PubMed: 23221344]
11. Collins S. A heart-adipose tissue connection in the regulation of energy metabolism. Nature Reviews Endocrinology. 2014; 10:157–163.
12. Mirbolooki MR, Upadhyay SK, Constantinescu CC, Pan M-L, Mukherjee J. Adrenergic pathway activation enhances brown adipose tissue metabolism: A [(18)F]FDG PET/CT study in mice. Nucl Med Biol. 2014; 41:10–16. [PubMed: 24090673]
13. Tam CS, Lecoultre V, Ravussin E. Brown adipose tissue: mechanisms and potential therapeutic targets. Circulation. 2012; 125:2782–2791. [PubMed: 22665886]
14. Bordicchia M, Liu D, Amri E-Z, Ailhaud G, Dessì-Fulgheri P, Zhang C, Takahashi N, Sarzani R, Collins S. Cardiac natriuretic peptides act via p38 MAPK to induce the brown fat thermogenic program in mouse and human adipocytes. J Clin Invest. 2012; 122:1022–1036. [PubMed: 22307324]
15. Cherenkov PA. Visible emission of clean liquids by action of γ radiation. Doklady Akademii Nauk SSSR. 1934
16. Thorek DLJ, Riedl CC, Grimm J. Clinical Cerenkov luminescence imaging of (18)F-FDG. J Nucl Med. 2014; 55:95–98. [PubMed: 24078721]
17. Hiremath P, Bauer M, Aguirre AD, Cheng H-W, Unno K, Patel RB, Harvey BW, Chang W-T, Groarke JD, Liao R, Cheng S. Identifying early changes in myocardial microstructure in hypertensive heart disease. PLoS ONE. 2014; 9:e97424. [PubMed: 24831515]
18. Huang S, Chen HH, Yuan H, Dai G, Schuhle DT, Mekkaoui C, Ngoy S, Liao R, Caravan P, Josephson L, Sosnovik DE. Molecular MRI of acute necrosis with a novel DNA-binding gadolinium chelate: kinetics of cell death and clearance in infarcted myocardium. Circulation: Cardiovascular Imaging. 2011; 4:729–737. [PubMed: 21836081]
19. Sosnovik DE, Garanger E, Aikawa E, Nahrendorf M, Figuiredo J-L, Dai G, Reynolds F, Rosenzweig A, Weissleder R, Josephson L. Molecular MRI of cardiomyocyte apoptosis with simultaneous delayed-enhancement MRI distinguishes apoptotic and necrotic myocytes in vivo: potential for midmyocardial salvage in acute ischemia. Circulation: Cardiovascular Imaging. 2009; 2:460–467. [PubMed: 19920044]
20. Panagia M, Chen Y-CI, Chen HH, Ernande L, Chen C, Chao W, Kwong K, Scherrer-Crosbie M, Sosnovik DE. Functional and anatomical characterization of brown adipose tissue in heart failure with blood oxygen level dependent magnetic resonance. NMR Biomed. 2016; 29:978–984. [PubMed: 27226402]
21. Qin F, Siwik DA, Pimentel DR, Morgan RJ, Biolo A, Tu VH, Kang YJ, Cohen RA, Colucci WS. Cytosolic H2O2 mediates hypertrophy, apoptosis, and decreased SERCA activity in mice with chronic hemodynamic overload. AJP: Heart and Circulatory Physiology. 2014; 306:H1453–63. [PubMed: 24633550]
22. Chen HH, Feng Y, Zhang M, Chao W, Josephson L, Shaw SY, Sosnovik DE. Protective effect of the apoptosis-sensing nanoparticle AnxCLIO-Cy5.5. Nanomedicine. 2012; 8:291–298. [PubMed: 21704591]
23. Kovacova Z, Tharp WG, Liu D, Wei W, Xie H, Collins S, Pratley RE. Adipose tissue natriuretic peptide receptor expression is related to insulin sensitivity in obesity and diabetes. Obesity. 2016; 24:820–828. [PubMed: 26887289]
24. Liew CW, Xu S, Wang X, McCann M, Whang Kong H, Carley AC, Pang J, Fantuzzi G, O'Donnell JM, Lewandowski ED. Multiphasic Regulation of Systemic and Peripheral Organ Metabolic Responses to Cardiac Hypertrophy. Circulation: Heart Failure. 2017; 10:e003864. [PubMed: 28404627]

25. Woong Hee Kim JLD-WJDRW. Visualizing Sweetness: Increasingly Diverse Applications for Fluorescent-Tagged Glucose Bioprobes and Their Recent Structural Modifications. PLoS ONE. 2012; 12:5005–5027.
26. Tseng J-C, Wang Y, Banerjee P, Kung AL. Incongruity of Imaging Using Fluorescent 2-DG Conjugates Compared to 18F-FDG in Preclinical Cancer Models. Mol Imaging Biol. 2012; 14:553–560. [PubMed: 22302178]
27. Virtanen KA, Lidell ME, Orava J, Heglind M, Westergren R, Niemi T, Taittonen M, Laine J, Savisto NJ, Enerbäck S. Functional brown adipose tissue in healthy adults. N Engl J Med. 2009; 360:1518–1525. [PubMed: 19357407]
28. Cypess AM, Lehman S, Williams G, Tal I, Rodman D, Goldfine AB, Kuo FC, Palmer EL, Tseng Y-H, Doria A, Kolodny GM, Kahn CR. Identification and Importance of Brown Adipose Tissue in Adult Humans. N Engl J Med. 2009; 360:1509–1517. [PubMed: 19357406]
29. Thoonen R, Ernande L, Cheng J, Nagasaka Y, Yao V, Miranda-Bezerra A, Chen C, Chao W, Panagia M, Sosnovik DE, Puppala D, Armoundas AA, Hindle A, Bloch KD, Buys ES, Scherrer-Crosbie M. Functional brown adipose tissue limits cardiomyocyte injury and adverse remodeling in catecholamine-induced cardiomyopathy. J Mol Cell Cardiol. 2015; 84:202–211. [PubMed: 25968336]
30. Hamilton G, Smith DL Jr, Bydder M, Nayak KS, Hu HH. MR properties of brown and white adipose tissues. J Magn Reson Imaging. 2011; 34:468–473. [PubMed: 21780237]
31. Garcia-Menendez L, Karamanlidis G, Kolwicz S, Tian R. Substrain specific response to cardiac pressure overload in C57BL/6 mice. AJP: Heart and Circulatory Physiology. 2013; 305:H397–402. [PubMed: 23709599]
32. Martin TP, Robinson E, Harvey AP, MacDonald M, Grieve DJ, Paul A, Currie S. Surgical optimization and characterization of a minimally invasive aortic banding procedure to induce cardiac hypertrophy in mice. Exp Physiol. 2012; 97:822–832. [PubMed: 22447975]
33. Bordicchia M, Pocognoli A, D'Anzeo M, Siquini W, Minardi D, Muzzonigro G, Dessì-Fulgheri P, Sarzani R. Nebivolol induces, via β3 adrenergic receptor, lipolysis, uncoupling protein 1, and reduction of lipid droplet size in human adipocytes. J Hypertens. 2014; 32:389–396. [PubMed: 24256707]
34. Valero-Muñoz M, Li S, Wilson RM, Hulsmans M, Aprahamian T, Fuster JJ, Nahrendorf M, Scherer PE, Sam F. Heart Failure With Preserved Ejection Fraction Induces Beiging in Adipose Tissue. Circulation: Heart Failure. 2016; 9:e002724. [PubMed: 26721917]
35. Wang W, Seale P. Control of brown and beige fat development. Nat Rev Mol Cell Biol. 2016; 17:691–702. [PubMed: 27552974]
36. McMillan AC, White MD. Induction of thermogenesis in brown and beige adipose tissues: molecular markers, mild cold exposure and novel therapies. Curr Opin Endocrinol Diabetes Obes. 2015; 22:347–352. [PubMed: 26313896]
37. Clark AL, Anker SD. Body mass, chronic heart failure, surgery and survival. J Heart Lung Transplant. 2010; 29:261–264. [PubMed: 19837608]
38. Taegtmeyer H, Lam T, Davogustto G. Cardiac Metabolism in Perspective. Compr Physiol. 2016; 6:1675–1699. [PubMed: 27783856]
39. Ingwall JS. Energy metabolism in heart failure and remodelling. Cardiovasc Res. 2009; 81:412–419. [PubMed: 18987051]
40. Lopaschuk GD, Ussher JR. Evolving Concepts of Myocardial Energy Metabolism. Circulation Research. 2016; 119:1173–1176. [PubMed: 28051784]
41. Nascimben L, Ingwall JS, Lorell BH, Pinz I, Schultz V, Tornheim K, Tian R. Mechanisms for increased glycolysis in the hypertrophied rat heart. Hypertension. 2004; 44:662–667. [PubMed: 15466668]
42. Lahey R, Wang X, Carley AN, Lewandowski ED. Dietary Fat Supply to Failing Hearts Determines Dynamic Lipid Signaling for Nuclear Receptor Activation and Oxidation of Stored Triglyceride. Circulation. 2014; 130:1790–1799. [PubMed: 25266948]
43. Labbé SM, Caron A, Bakan I, Laplante M, Carpentier AC, Lecomte R, Richard D. In vivo measurement of energy substrate contribution to cold-induced brown adipose tissue thermogenesis. FASEB J. 2015; 29:2046–2058. [PubMed: 25681456]

44. Kajimura S, Seale P, Spiegelman BM. Transcriptional Control of Brown Fat Development. Cell Metabolism. 2010; 11:257–262. [PubMed: 20374957]

45. Forner F, Kumar C, Luber CA, Fromme T, Klingenspor M, Mann M. Proteome differences between brown and white fat mitochondria reveal specialized metabolic functions. Cell Metabolism. 2009; 10:324–335. [PubMed: 19808025]

46. Bottomley PA, Panjrath GS, Lai S, Hirsch GA, Wu K, Najjar SS, Steinberg A, Gerstenblith G, Weiss RG. Metabolic rates of ATP transfer through creatine kinase (CK Flux) predict clinical heart failure events and death. Sci Transl Med. 2013; 5:215re3–215re3.

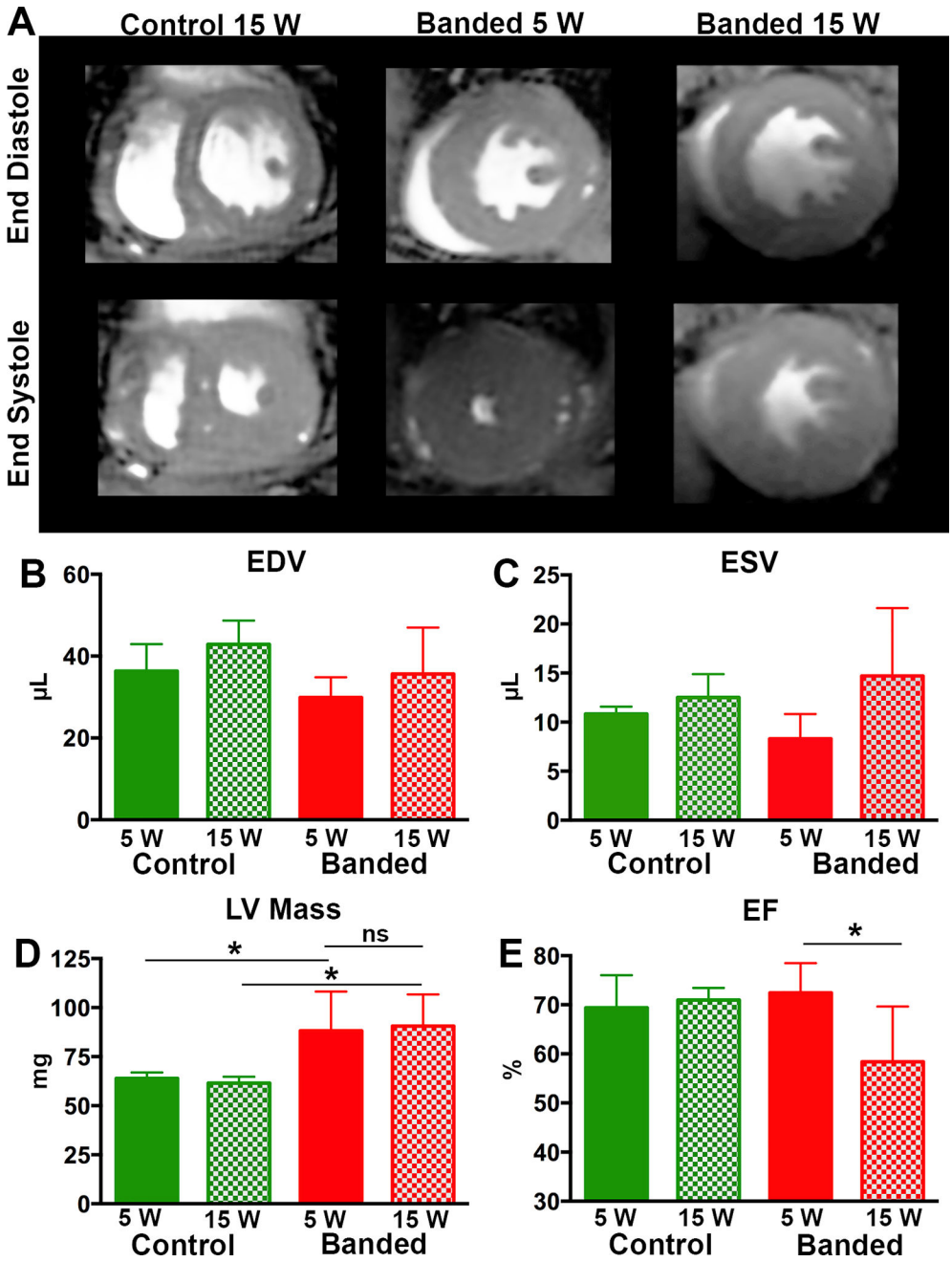

Figure 1. Progressive Cardiac Dysfunction with Prolonged TAC

(A) Cardiac MRI images showing a mid-ventricular slice at end diastole and end systole for control, 5 weeks post TAC and 15 weeks post TAC mice. EDV (B) and ESV (C). LV mass was increased, compared to controls, at both 5 and 15 weeks but no difference in LV mass was seen between the banded animals at the 5 and 15 week time points (D). However, a significant decrease in ejection fraction (E) was seen at 15 weeks post TAC. (* $p < 0.05$).

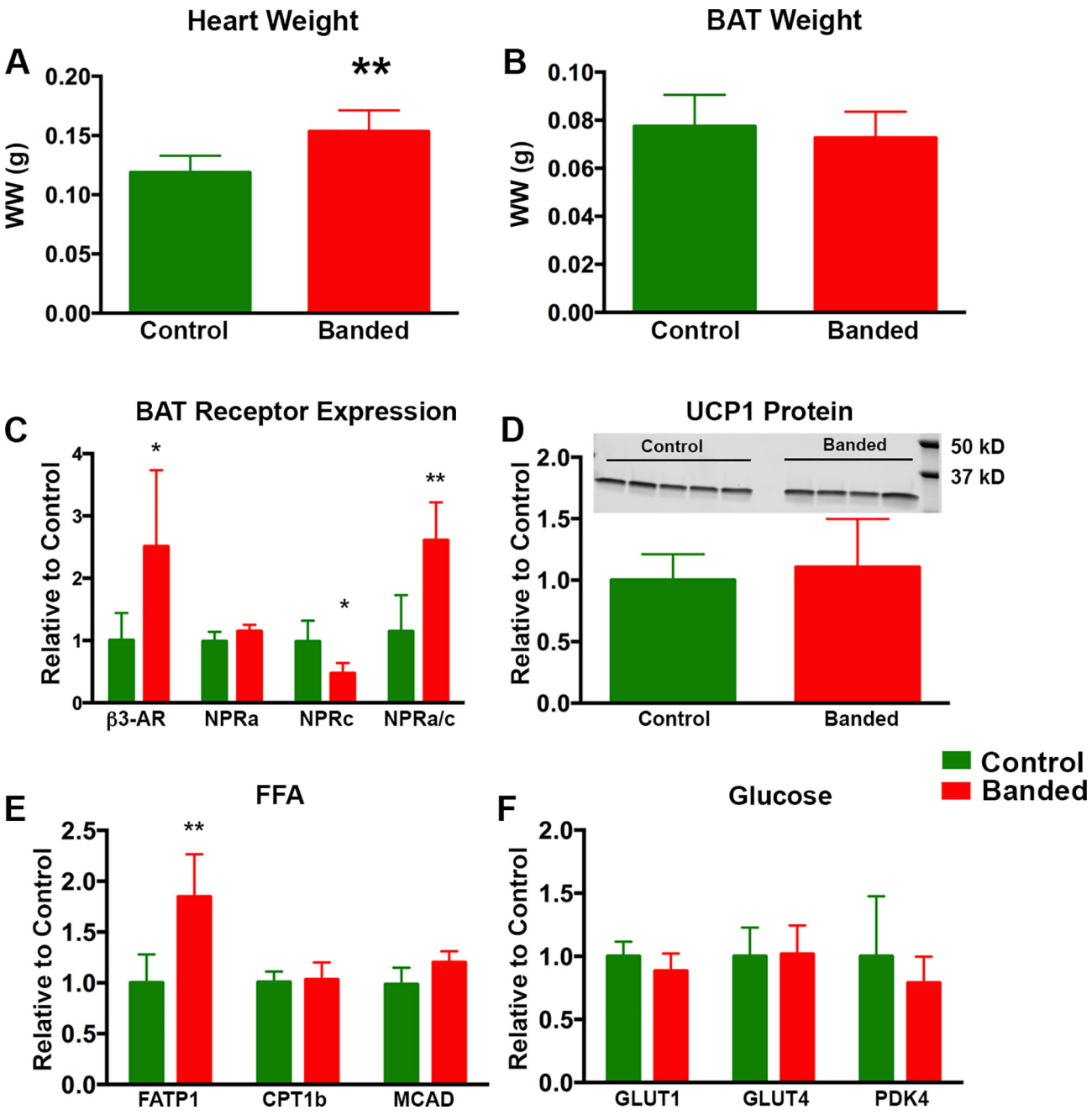

Figure 2. BAT Morphology and Activation State 5 Weeks Post TAC

At 5 weeks post TAC there was a significant increase in heart wet weight in banded animals (A) but no significant difference in BAT wet weight (B). In BAT from banded animals there was a significant increase in β_3AR mRNA. Although there was no change in the NPRa levels, there was a significant decrease in NPRc receptor levels leading to a significantly increased NPRa/c ratio (C). UCP1 protein levels (D) were unchanged between groups at 5 weeks (normalized to α-tubulin which was unchanged between groups). There was a significant increase in FATP1 but remaining key enzymes involved in FFA uptake and

metabolism were unchanged (E) and key enzymes in glucose uptake and metabolism (F) also remained unchanged. (* $p < 0.05$, ** $p < 0.01$, *** $p < 0.001$).

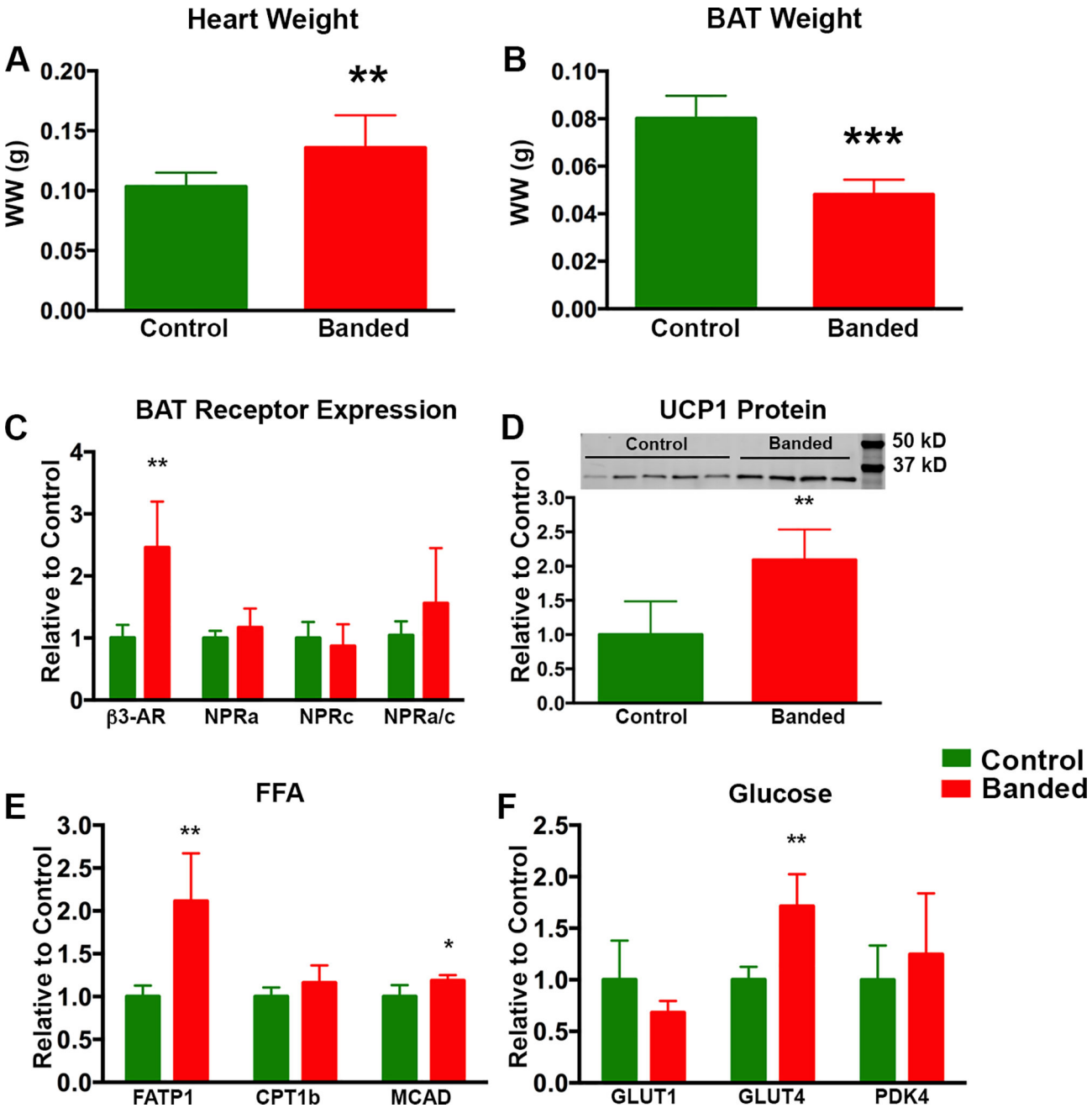

Figure 3. BAT Morphology and Activation State 15 Weeks Post TAC

At 15 weeks post TAC there was a significant increase in heart wet weight (A) and a significant decrease in BAT wet weight (B) in banded vs control animals. In BAT from banded animals there was a significant increase in β_3AR mRNA however, there was no significant change in the NPRa or NPRc receptor levels (C). Although a trend towards an increased NPRa/c ratio remained present, it was not significant. Unlike the 5 week time point, UCP1 protein levels (D) were significantly increased in the banded animals at 15 weeks (normalized to α-tubulin which was unchanged between groups). There was a significant increase in both FATP1 and MCAD mRNA between the two groups and a trend

towards increased CPT1B (E). Transcript levels of GLUT1 and PDK4 were unchanged between the two groups at 15 weeks post TAC, however there was a significant increase in GLUT4 mRNA in the BAT of banded vs control animals. (* $p < 0.05$, ** $p < 0.01$, *** $p < 0.001$).

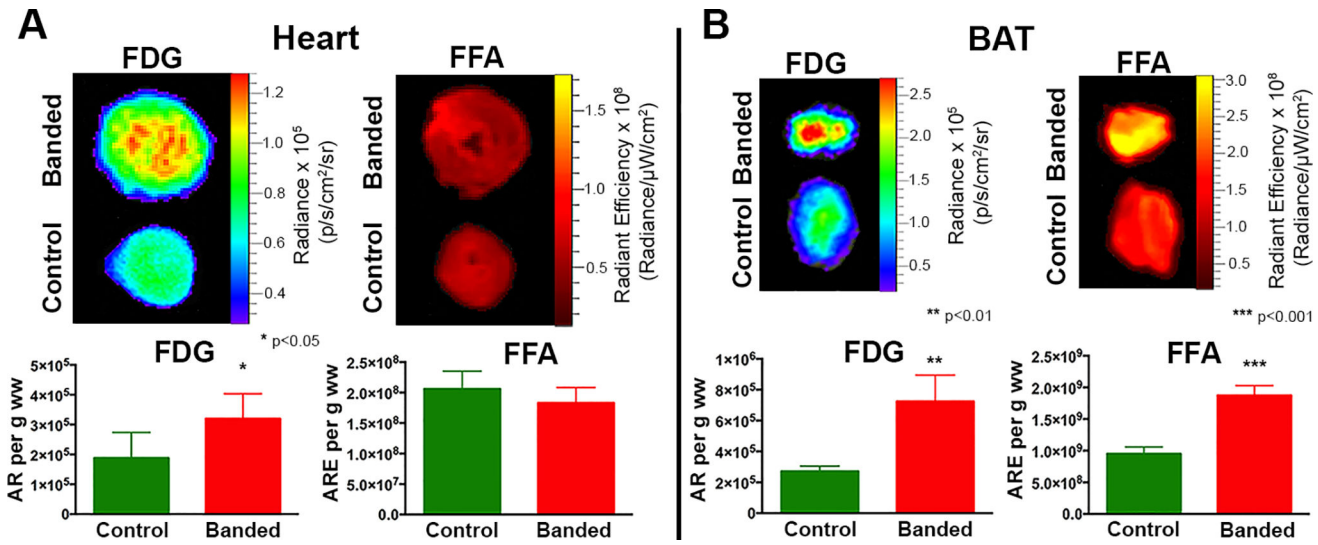

Figure 4. Multiplexed Optical Imaging of Substrate Uptake in the Heart and BAT 15 Weeks Post TAC

(A) Simultaneous CLI and FRI of glucose and FFA substrate uptake in the heart, 15 weeks post TAC, show a significant increase in glucose uptake and a trend towards decreased FFA uptake. (B) In BAT, significant increases in both glucose and FFA uptake are seen in the banded mice. (*p< 0.05, **p <0.01, ***p<0.001).

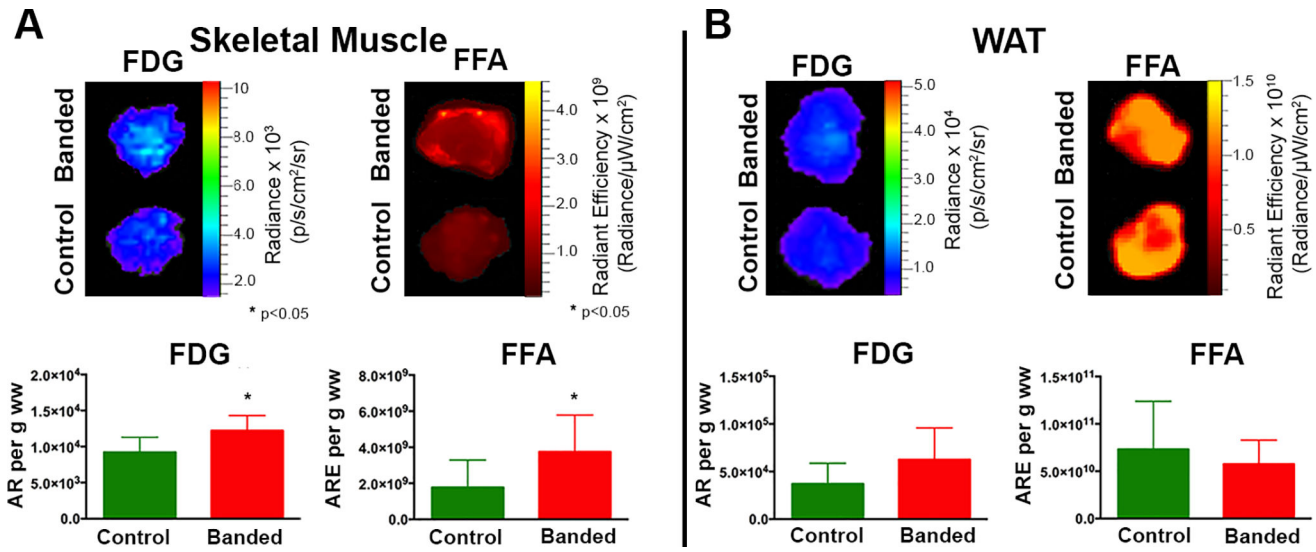

Figure 5. Multiplexed Optical Imaging of Substrate Uptake in the Skeletal Muscle and WAT 15 Weeks Post TAC

Glucose and FFA uptake are increased in the skeletal muscle of banded animals compared to control animals (A) but there is no difference in substrate uptake between the two groups in WAT (B). (* $p < 0.05$).

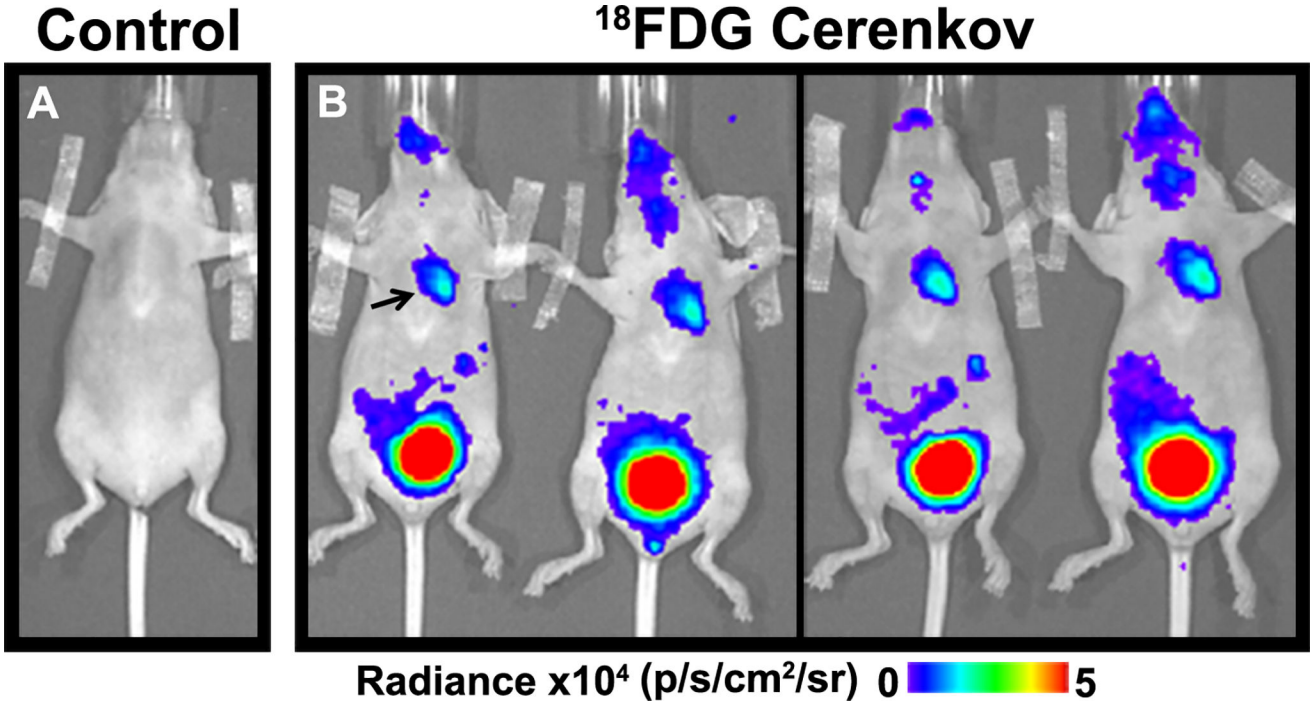

Figure 6. Cerenkov luminescence imaging of the Heart *in vivo* with ^{18}F-FDG

(A) No signal was seen in the thorax after saline injection. (B). Robust signal in the thorax (arrow) was seen in the mice injected with FDG, consistent with glucose uptake in the heart. Renal excretion of the probe resulted in an extremely strong signal from the bladder.

Table

Tissue Specific Metabolic Patterns in Response to Prolonged LVH

	Glucose Uptake	FFA Uptake
Myocardium	↑	-
BAT	↑↑↑	↑↑
WAT	-	-
Skeletal Muscle	↑	↑↑